

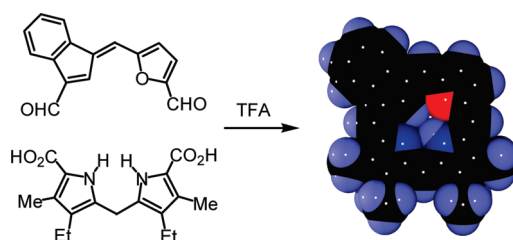
Preparation of Furan and Thiophene-Derived Fulvene Dialdehydes: Synthesis and Structural Characterization of a 22-Oxa-21- carbaporphyrin and a Related Palladium(II) Organometallic Complex[†]

Pankaj Jain, Gregory M. Ferrence, and Timothy D. Lash*

Department of Chemistry, Illinois State University, Normal, Illinois 61790-4160

tdlash@ilstu.edu

Received July 4, 2010



A series of fulvene monoaldehydes were prepared by reacting furan or thiophene carbaldehydes with an indene-derived enamine in the presence of *di-n*-butylboron triflate, but considerable difficulties were encountered in the preparation of fulvene dialdehydes needed for the synthesis of novel porphyrin analogues. These problems were overcome by reacting protected iodofulvenes with magnesium ate complexes at low temperatures, followed by addition of DMF and hydrolysis. The thiophene-containing fulvene gave good yields of the dialdehyde at $-78\text{ }^{\circ}\text{C}$ or $-100\text{ }^{\circ}\text{C}$, but the furan system gave a major byproduct formally derived from valeraldehyde under the higher temperature conditions. This compound was fully characterized by NMR spectroscopy, mass spectrometry, and X-ray crystallography. However, this side reaction could be completely avoided at $-100\text{ }^{\circ}\text{C}$, and the required furan-containing fulvene dialdehyde was isolated in 46% yield. The furan-derived dialdehyde reacted with a dipyrromethane in the presence of trifluoroacetic acid to give the 22-oxa-21-carbaporphyrin **19** in excellent yields (73–79%). However, the thiophene-containing fulvene dialdehyde failed to give any of the anticipated macrocyclic product. An unstable acyclic intermediate was isolated and partially characterized, but this species could not be induced to cyclize. Steric factors may play a role, but X-ray crystallography confirmed that the fulvene dialdehyde precursor does have the correct geometry to facilitate the formation of the porphyrinoid macrocycle. The new oxacarbaporphyrin was fully characterized and could easily be converted into the corresponding mono- and dicationic species. The second protonation involves addition onto the internal indene carbon and proton NMR spectroscopy for the sample in HCl–TFA demonstrates that it retains strongly diatropic characteristics. The free base oxacarbaporphyrin reacted with $\text{Pd}(\text{OAc})_2$ in DMF to give the corresponding palladium(II) organometallic derivative **27**. The proton NMR spectrum for this complex also shows the retention of a strong, albeit slightly reduced, diatropic ring current. The free base oxacarbaporphyrin and the palladium derivative were both structurally characterized by X-ray crystallography. The bond lengths for **19** and **27** were consistent with the presence of significant 18π -electron delocalization pathways.

Introduction

The discovery of N-confused porphyrins (**1**)^{1–3} and related carbaporphyrinoid systems **2–5**^{4–10} (Figure 1) in the

mid-1990s attracted widespread attention due in part to the insightful contrasts they provide with true porphyrins. Carbaporphyrinoid systems of this type were shown to have

[†] Part 55 in the series “Conjugated Macrocycles Related to the Porphyrins”. For part 54, see: Lash, T. D.; Jones, S. A.; Ferrence, G. M. *J. Am. Chem. Soc.* 2010, published ASAP August 25, 2010; DOI: 10.1021/ja105146a.

(1) (a) Furuta, H.; Asano, T.; Ogawa, T. *J. Am. Chem. Soc.* **1994**, *116*, 767–768. (b) Chmielewski, P. J.; Latos-Grazynski, L.; Rachlewicz, K.; Glowinski, T. *Angew. Chem., Int. Ed. Engl.* **1994**, *33*, 779–781.

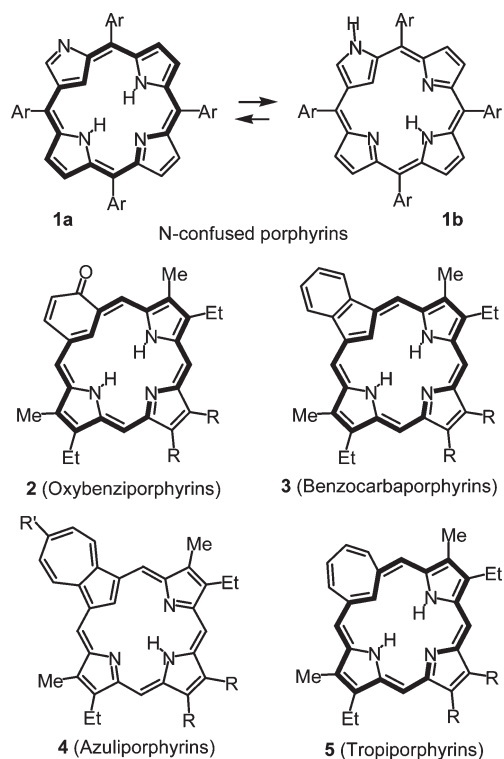


FIGURE 1. N-Confused porphyrins and related carbaporphyrinoid systems.

unique chemical properties, including the ability to form stable organometallic derivatives under mild conditions^{11,12} or undergo selective oxidation reactions.¹³ These observations

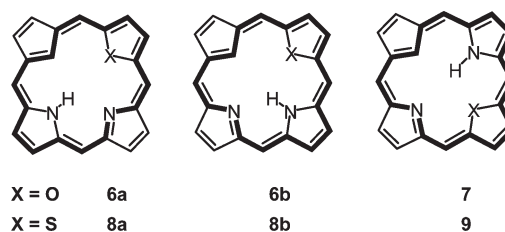


FIGURE 2. Oxa- and thiacarbazoporphyrrins.

soon led to speculation about the properties of related porphyrinoid systems with chalcogenide atoms replacing one or more nitrogens of a given carbaporphyrinoid species.¹⁴ Theoretical studies were directed at rationalizing and predicting the metalation properties of these organometallic ligands, in assessing the favorability of tautomeric species, and in predicting the bond lengths for these structures.^{14,15} Oxa- and thiacarbazoporphyrrins **6–9** (Figure 2) were assessed using DFT techniques.¹⁴ For the oxa-series, the *adj*-oxacarbazoporphyrrin system **6** was predicted to be 6–7 kcal/mol more stable than the *opp*-isomer **7**; in addition tautomer **6a** was calculated to be 1 kcal/mol more stable than tautomer **6b**.¹⁴ In the thia-series, the *opp*-isomer **9** is predicted to be the more stable than *adj*-thiacarbazoporphyrrin **8**. Tautomer **8a** was calculated to be the more stable form with a relative energy compared to **9** of 3 kcal/mol, whereas the less stable tautomer **8b** gave a value that was 6 kcal/mol higher than **9**.¹⁴ Although *opp*-oxa-, thia-, and seleno-N-confused porphyrins were synthesized some time ago,^{16,17} the synthesis of *adj*-hetero N-confused porphyrins has proven to be far more challenging.¹⁸ However, carbaporphyrinoid systems with two furan or thiophene rings have been noted.^{19–21} Examples of *opp*-hetero carbaporphyrinoids, including benzocarbazoporphyrrins, azuliporphyrins, and oxybenzoporphyrrins, were also reported using the “3 + 1” variant

(2) (a) Latos-Grazynski, L. *Core Modified Heteroanalogues of Porphyrins and Metalloporphyrins*. In *The Porphyrin Handbook*; Kadish, K. M., Smith, K. M., Guillard, R., Eds.; Academic Press: San Diego, 2000; Vol. 2, pp 361–416. (b) Srinivasan, A.; Furuta, H. *Acc. Chem. Res.* **2005**, *38*, 10–20. (c) Harvey, J. D.; Ziegler, C. J. *Coord. Chem. Rev.* **2003**, *247*, 1–19.

(3) (a) Liu, B. Y.; Brückner, C.; Dolphin, D. *Chem. Commun.* **1996**, 2141–2142. (b) Lash, T. D.; Richter, D. T.; Shiner, C. M. *J. Org. Chem.* **1999**, *64*, 7973–7982. (c) Lash, T. D.; Von Ruden, A. L. *J. Org. Chem.* **2008**, *73*, 9417–9425.

(4) (a) Lash, T. D. *Synlett* **2000**, 279–295. (b) Lash, T. D. *Eur. J. Org. Chem.* **2007**, 5461–5481.

(5) Lash, T. D. *Synthesis of Novel Porphyrinoid Chromophores*. In *The Porphyrin Handbook*; Kadish, K. M., Smith, K. M., Guillard, R., Eds.; Academic Press: San Diego, 2000; Vol. 2, pp 125–199.

(6) Oxybenzoporphyrrins: (a) Lash, T. D. *Angew. Chem., Int. Ed. Engl.* **1995**, *34*, 2533–2535. (b) Lash, T. D.; Chaney, S. T.; Richter, D. T. *J. Org. Chem.* **1998**, *63*, 9076–9088. (c) Richter, D. T.; Lash, T. D. *Tetrahedron* **2001**, *57*, 3659–3673. (d) Stepien, M.; Latos-Grazynski, L.; Lash, T. D.; Sztrenberg, L. *Inorg. Chem.* **2001**, *40*, 6892–6900. (e) Miyake, K.; Lash, T. D. *Chem. Commun.* **2004**, 178–179. (f) El-Beck, J. A.; Lash, T. D. *Org. Lett.* **2006**, *8*, 5263–5266.

(7) Carbazoporphyrrins: (a) Lash, T. D.; Hayes, M. J. *Angew. Chem., Int. Ed. Engl.* **1997**, *36*, 840–842. (b) Berlin, K. *Angew. Chem., Int. Ed. Engl.* **1996**, *35*, 1820–1821. (c) Lash, T. D. *Chem. Commun.* **1998**, 1683–1684. (d) Lash, T. D.; Hayes, M. J.; Spence, J. D.; Muckey, M. A.; Ferrence, G. M.; Szczepura, L. F. *J. Org. Chem.* **2002**, *67*, 4860–4874. (e) Liu, D.; Lash, T. D. *J. Org. Chem.* **2003**, *68*, 1755–1761.

(8) Azuliporphyrins: (a) Lash, T. D.; Chaney, S. T. *Angew. Chem., Int. Ed. Engl.* **1997**, *36*, 839–840. (b) Graham, S. R.; Colby, D. A.; Lash, T. D. *Angew. Chem., Int. Ed.* **2002**, *41*, 1371–1374. (c) Colby, D. A.; Lash, T. D. *Chem.—Eur. J.* **2002**, *8*, 5397–5402. (d) Lash, T. D.; Colby, D. A.; Ferrence, G. M. *Eur. J. Org. Chem.* **2003**, 4533–4548. (e) Lash, T. D.; Colby, D. A.; Graham, S. R.; Chaney, S. T. *J. Org. Chem.* **2004**, *69*, 8851–8864. (f) Lash, T. D.; El-Beck, J. A.; Ferrence, G. M. *J. Org. Chem.* **2007**, *72*, 8402–8415. (g) El-Beck, J. A.; Lash, T. D. *Eur. J. Org. Chem.* **2007**, 3981–3990.

(9) Tropiporphyrins: (a) Lash, T. D.; Chaney, S. T. *Tetrahedron Lett.* **1996**, *37*, 8825–8828. (b) Bergman, K. M.; Ferrence, G. M.; Lash, T. D. *J. Org. Chem.* **2004**, *69*, 7888–7897.

(10) Carbachlorins: Hayes, M. J.; Lash, T. D. *Chem.—Eur. J.* **1998**, *4*, 508–511.

(11) (a) Graham, S. R.; Ferrence, G. M.; Lash, T. D. *Chem. Commun.* **2002**, 894–895. (b) Lash, T. D.; Colby, D. A.; Graham, S. R.; Ferrence, G. M.; Szczepura, L. F. *Inorg. Chem.* **2003**, *42*, 7326–7338.

(12) (a) Muckey, M. A.; Szczepura, L. F.; Ferrence, G. M.; Lash, T. D. *Inorg. Chem.* **2002**, *41*, 4840–4842. (b) Lash, T. D.; Colby, D. A.; Szczepura, L. F. *Inorg. Chem.* **2004**, *43*, 5258–5267. (c) Lash, T. D.; Rasmussen, J. M.; Bergman, K. M.; Colby, D. A. *Org. Lett.* **2004**, *6*, 549–552.

(13) (a) Lash, T. D.; Muckey, M. A.; Hayes, M. J.; Liu, D.; Spence, J. D.; Ferrence, G. M. *J. Org. Chem.* **2003**, *68*, 8558–8570. (b) Colby, D. A.; Ferrence, G. M.; Lash, T. D. *Angew. Chem., Int. Ed.* **2004**, *43*, 1346–1349. (c) Furuta, H.; Maeda, A.; Osuka, A. *Org. Lett.* **2002**, *4*, 181–184. (d) Pawlicki, M.; Kanska, I.; Latos-Grazynski, L. *Inorg. Chem.* **2007**, *46*, 6575–6584.

(14) Ghosh, A.; Wondimagn, T.; Nilsen, H. J. *J. Phys. Chem. B* **1998**, *102*, 10459–10467.

(15) Ghosh, A. *Angew. Chem., Int. Ed. Engl.* **1995**, *34*, 1028–1029.

(16) (a) Heo, P.-Y.; Lee, C.-H. *Bull. Korean Chem. Soc.* **1996**, *17*, 515–520. (b) Lee, C.-H.; Kim, H.-J. *Tetrahedron Lett.* **1997**, *38*, 3935–3938. (c) Lee, C.-H.; Kim, H.-J.; Yoon, D.-W. *Bull. Korean Chem. Soc.* **1999**, *20*, 276–280.

(17) Pushpan, S. K.; Srinivasan, A.; Anand, V. R. G.; Chandrashekar, T. K.; Subramanian, A.; Roy, R.; Sugiura, K.-i.; Sakata, Y. *J. Org. Chem.* **2001**, *66*, 153–161.

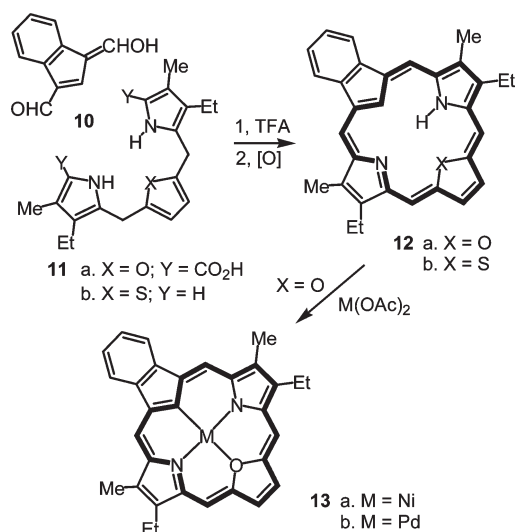
(18) Pacholska, E.; Latos-Grazynski, L.; Sztrenberg, L.; Ciunik, Z. *J. Org. Chem.* **2000**, *65*, 8188–8196.

(19) Sprutta, N.; Latos-Grazynski, L. *Org. Lett.* **2001**, *3*, 1933–1936.

(20) For macrocycles with alternating azulene and thiophene or furan rings, see: (a) Sprutta, N.; Swiderska, M.; Latos-Grazynski, L. *J. Am. Chem. Soc.* **2005**, *127*, 13108–13109. (b) Sprutta, N.; Siczek, M.; Latos-Grazynski, L.; Pawlicki, M.; Sztrenberg, L.; Lis, T. *J. Org. Chem.* **2007**, *72*, 9501–9509.

(21) For relevant reviews on the synthesis and coordination chemistry of core modified porphyrinoids, see: (a) Pushpan, S. K.; Venkatraman, S.; Anand, V. G.; Sankar, J.; Rath, H.; Chandrashekar, T. K. *Proc. Indian Acad. Sci. (Chem. Sci.)* **2002**, *114*, 311–338. (b) Pushpan, S. K.; Chandrashekar, T. K. *Pure Appl. Chem.* **2002**, *74*, 2045–2055. (c) Chmielewski, P. J.; Latos-Grazynski, L. *Coord. Chem. Rev.* **2005**, *249*, 2510–2533. (d) Gupta, I.; Ravikanth, M. *Coord. Chem. Rev.* **2006**, *250*, 468–518.

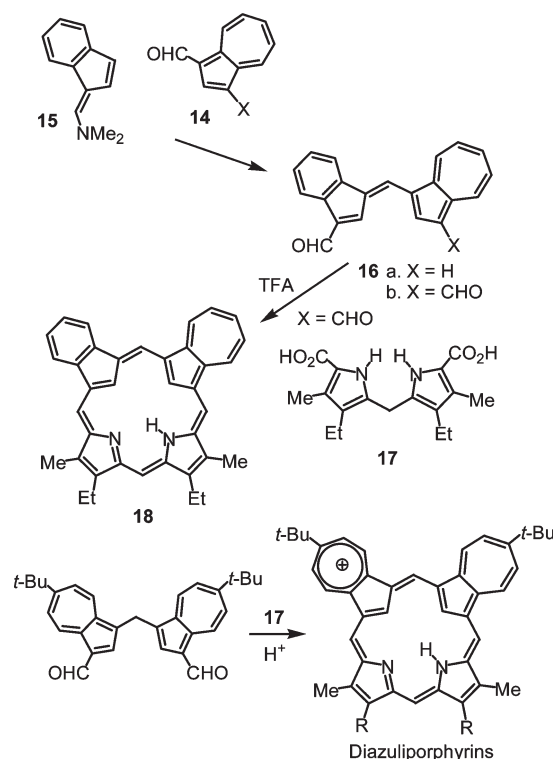
SCHEME 1



of the MacDonald condensation.^{8b,c,22–24} For instance, indene dialdehyde **10** reacted with oxa- and thiatripyrranes **11** in the presence of TFA in dichloromethane to give, following oxidation with DDQ, the corresponding oxa- and thiabenzocarbaporphyrins **12** (Scheme 1).^{22,23} These porphyrin analogues are essentially substituted versions of **7** and **9**; the fused benzo-unit is almost always present in synthetic carbaporphyrins due in part to the availability of suitable synthetic intermediates.⁷ Oxabenzocarbaporphyrin **12a** proved to be a dianionic ligand, readily forming organometallic derivatives **13** with nickel(II) or palladium(II) acetate.^{23,25} This contrasts with benzocarbaporphyrins **3**, which are trianionic ligands that form stable silver(III) derivatives.¹²

Although the formation of *opp*-hetero carbaporphyrins has been well established, no reports on the preparation of carbaporphyrins with adjacent furan or thiophene subunits have appeared in the literature. The elusiveness of the *adj*-hetero carbaporphyrin series is primarily due to the need for new synthetic procedures to generate porphyrin analogue systems. Recently, we reported the first synthesis of an *adj*-dicarbaporphyrinoid using a fulvene dialdehyde as the key intermediate.²⁶ Azulene aldehydes **14** were shown to react with indene-derived enamine **15** in the presence of *n*-Bu₂BOTf to give fulvenes **16** in good yields (Scheme 2).²⁶ When the reaction was performed using dialdehyde **14b**, the required fulvene dialdehyde **16b** was generated.²⁶ This underwent an acid-catalyzed condensation with dipyrromethane **17**

SCHEME 2



to give 22-carbaazulporphyrin **18**.^{26–28} A similar “2 + 2” approach was also applied to the synthesis of *adj*-diazulporphyrins (Scheme 2).²⁹ In principle, the fulvene dialdehyde strategy provides a suitable methodology for synthesizing other porphyrin analogues with two adjacent nonpyrrolic subunits. In this paper, we report the preparation of a series of furan and thiophene-derived fulvene aldehydes. These were utilized to explore the synthesis of the first examples of *adj*-hetero carbaporphyrins.

Results and Discussion

Oxa- and thiabenzocarbaporphyrins **19** and **20**, respectively, were targeted for synthesis. It was anticipated that these novel porphyrin analogues could be prepared from fulvene dialdehydes **21** and **22**, together with the readily available dipyrromethane **17**³⁰ using the MacDonald “2 + 2” approach³¹ (Scheme 3). Attempts to prepare fulvene dialdehydes in one step from benzenedicarbaldehydes had failed in related studies,³² and it seemed prudent to develop a more step-wise route for the preparation of **21** and **22**. Fulvene monoaldehydes **23a–f** were easily prepared by reacting enamine **15** with a series of furan and thiophenecarbaldehydes in the presence of *n*-Bu₂BOTf in dichloromethane (Scheme 4). Following hydrolysis with a saturated aqueous sodium acetate solution,

(22) Liu, D.; Lash, T. D. *Chem. Commun.* **2002**, 2426–2427.

(23) Liu, D.; Ferrence, G. M.; Lash, T. D. *J. Org. Chem.* **2004**, *69*, 6079–6093.

(24) (a) Venkatraman, S.; Anand, V. G.; Pushpan, S. K.; Sankar, J.; Chandrashekar, T. K. *Chem. Commun.* **2002**, 462–463. (b) Venkatraman, S.; Anand, V. G.; PrabhuRaja, V.; Rath, H.; Sankar, J.; Chandrashekar, T. K.; Teng, W.; Senge, K. R. *Chem. Commun.* **2002**, 1660–1661.

(25) The platinum(II) derivative was also prepared but could only be isolated in 5% yield.²³

(26) Lash, T. D.; Colby, D. A.; Idate, A. S.; Davis, R. N. *J. Am. Chem. Soc.* **2007**, *129*, 13800–13801.

(27) Syntheses of *opp*-dicarbaporphyrins are more established. (a) Lash, T. D.; Romanic, J. L.; Hayes, M. J.; Spence, J. D. *Chem. Commun.* **1999**, 819–820. (b) Xu, L.; Lash, T. D. *Tetrahedron Lett.* **2006**, *47*, 8863–8866. See also reference 8b. For an innovative new synthesis of an expanded porphyrin with two indene units, see: Peterson, G. R.; Bampos, N. *Angew. Chem., Int. Ed.* **2010**, *49*, 3930–3933.

(28) Syntheses of *adj*- and *opp*-doubly N-confused porphyrins have also been published: Furuta, H.; Maeda, H.; Osuka, A. *J. Am. Chem. Soc.* **2000**, *122*, 803–807. (b) Maeda, H.; Osuka, A.; Furuta, H. *J. Am. Chem. Soc.* **2003**, *125*, 15690–15691.

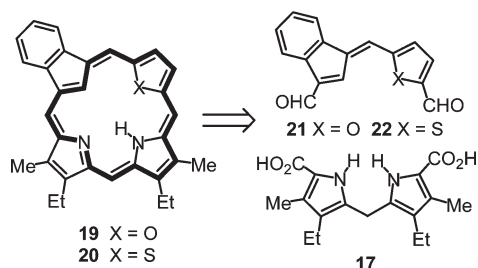
(29) Zhang, Z.; Ferrence, G. M.; Lash, T. D. *Org. Lett.* **2009**, *11*, 101–104.

(30) Lash, T. D.; Armiger, Y. L. S. T. *J. Heterocycl. Chem.* **1991**, *28*, 965–970.

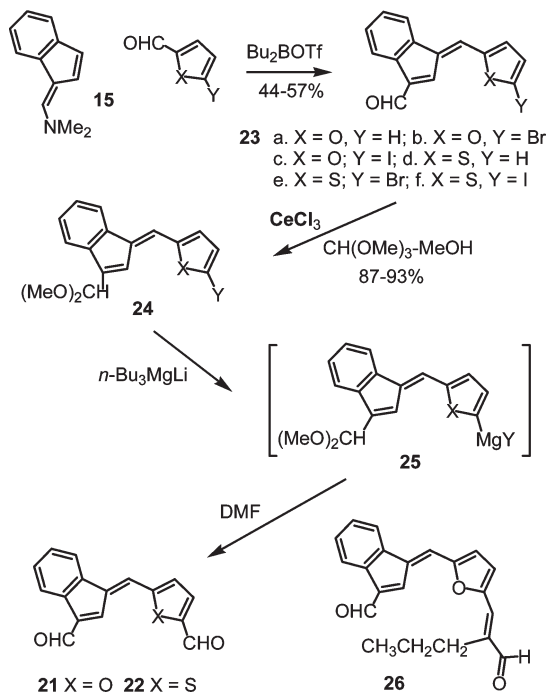
(31) Lash, T. D. *Chem.—Eur. J.* **1996**, *2*, 1197–1200.

(32) Although benzenedicarbaldehydes failed to give fulvene monoaldehydes with enamine **15**, stable difulvene derivatives could be isolated. See: Davis, R. N.; Lash, T. D. *Tetrahedron* **2009**, *65*, 9935–9943.

SCHEME 3



SCHEME 4



purification by column chromatography, and recrystallization, the heterocyclic fulvenes were isolated in 44–57% yield. Initially, fulvene **23a** was investigated as a potential precursor to dialdehyde **21**. However, attempts to introduce a second aldehyde moiety using Vilsmeier–Haack conditions failed to give any of the required product. Nevertheless, it was anticipated that metalation could be carried out on the furan ring and subsequent reaction with DMF would then give the required dialdehyde. To this end, the monoaldehyde **23a** was converted into the corresponding acetal **24a** in 93% yield by treating it with trimethyl orthoformate and methanol in the presence of cerium trichloride. However, numerous attempts to carry out direct metalation onto the furan unit using *n*-butyllithium or *tert*-butyllithium failed to give any metalated product. For this reason, the corresponding bromo- and iodo-fulvenes **23b** and **21c** were investigated. Again, the monoaldehydes were protected as the dimethyl acetals, and metal–halogen exchange was attempted using *n*-butyllithium or *tert*-butyllithium. Unfortunately, no reaction occurred under any of the conditions investigated. Attempts to directly generate the corresponding Grignard reagent were also unsuccessful.

Although metal–halogen exchange reactions had failed in our hands for fulvene derivatives **23b** and **23c**, alternative

procedures have been developed for other systems where difficulties of this type had arisen. Specifically, magnesium ate complexes have been shown to greatly increase reactivity. Synthetic applications of magnesium ate reagents had been little explored until recently, but these complexes have shown efficient halogen–magnesium exchange for various organic compounds and commonly give greatly increased reactivity.^{33–39} These studies often make use of a tri-*n*-butylmagnesium ate complex (*n*-Bu₃MgLi), and the reaction of suitably halogenated fulvenes with this reagent was considered to be a potentially viable method for preparing fulvene dialdehydes. *n*-Bu₃MgLi was prepared by reacting 2 equiv of a 1.6 M solution of *n*-butyllithium in hexanes with a 2.0 M solution of *n*-butylmagnesium chloride in THF and diethyl ether at 0 °C. The temperature was then lowered to between –78 and –100 °C, and the protected bromofulvene **24b** was slowly added to the stirred mixture. However, these conditions still did not give rise to metalation of the furan ring. Iodofulvene **24c** was also investigated, and this showed for the first time that these systems could be metalated. Fulvene acetal **24c** was reacted with *n*-Bu₃MgLi at –78 °C to form magnesium ate complex **25** and further treated with DMF. Following column chromatography and recrystallization, the required dialdehyde **21** was isolated in 23% yield. However, an unexpected dialdehyde byproduct was also generated (Scheme 4). The proton NMR spectrum of this byproduct was very similar to that of fulvene dialdehyde **21** but gave an additional singlet in the aromatic region and resonances showing the presence of a propyl group in the aliphatic region. Further characterization of this compound using ¹H and ¹³C NMR spectroscopy and mass spectrometry showed that the side product was the α,β -unsaturated aldehyde **26**. This compound is formally the crossed aldol condensation product formed from **21** and valeraldehyde. Valeraldehyde can be formed by reaction of DMF with *n*-butyllithium, but the origin of this side product is unclear. The structure was further confirmed by X-ray crystallography (Figure 3), and the alkene unit was thereby shown to have the expected *E*-geometry. Addition of an excess of *n*-butyllithium and higher temperature conditions (> –70 °C) increased the proportion of the undesired side product **26**. However, the selectivity of the reaction was increased when the temperature was lowered from –78 to –100 °C. Under these conditions, no formation of **26** was observed, and the yields of the required dialdehyde **137** were raised to 46%. The synthesis of a thiophene-derived fulvene dialdehyde **22** was also investigated. Again, monoaldehydes **23d–f** were protected as the dimethyl acetals **24d–f** and metalation reactions were attempted using *n*-butyl- or *tert*-butyllithium (Scheme 4). No metalation occurred under any of the conditions studied using these reagents, and for this

(33) Iida, T.; Wada, T.; Tomimoto, K.; Mase, T. *Tetrahedron Lett.* **2001**, 42, 4841–4844.

(34) Ito, S.; Kubo, T.; Morita, N.; Matsui, Y.; Watanabe, T.; Ohta, A.; Fujimori, K.; Murafuji, T.; Sugihara, Y.; Tajiri, A. *Tetrahedron Lett.* **2004**, 45, 2891–2894.

(35) Böhm, V. P. W.; Schulze, V.; Brönstrup, M.; Müller, M.; Hoffmann, R. W. *Organometallics* **2003**, 22, 2925–2930.

(36) Seitz, L. M.; Brown, T. L. *J. Am. Chem. Soc.* **1996**, 118, 4140–4147.

(37) Dumouchel, S.; Mongin, F.; Trécourt, F.; Quéguiner, G. *Tetrahedron* **2003**, 59, 8629–8640.

(38) Hatano, M.; Matsumura, T.; Ishihara, K. *Org. Lett.* **2005**, 7, 573–576.

(39) Inoue, A.; Kitagawa, K.; Shinokubo, H.; Oshima, K. *J. Org. Chem.* **2001**, 66, 4333–4339.

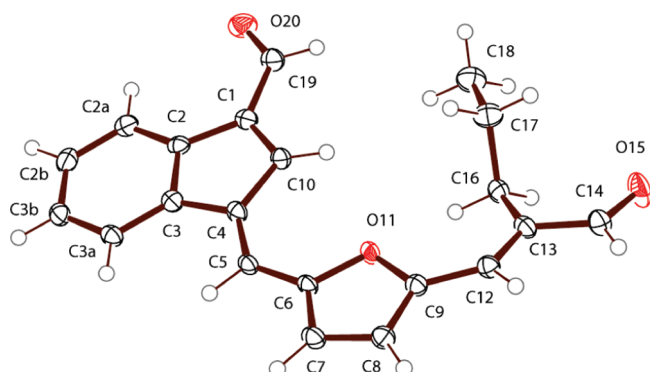
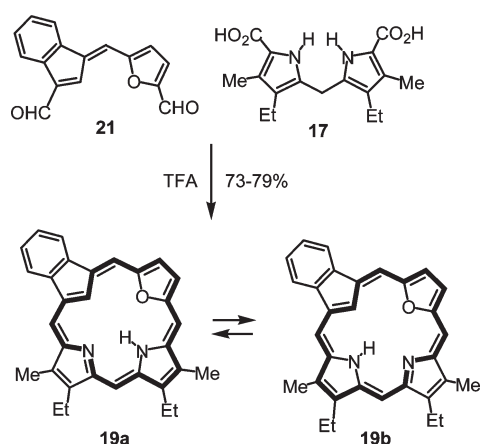


FIGURE 3. ORTEP III drawing (50% probability level, hydrogen atoms drawn arbitrarily small) of fulvene dialdehyde byproduct **26**.

SCHEME 5



reason the use of magnesium ate reagents was investigated for the thiophene series. Although no metal–halogen exchange was observed in reactions of bromofulvene **24e** with *n*-Bu₃MgLi, the iododerivative **24f** was well suited for this conversion. Reaction of **24f** with *n*-Bu₃MgLi at -78 or -100 °C, followed by addition of DMF and hydrolysis, gave dialdehyde **22** in up to 63% yield. Interestingly, side reactions to give byproduct like **26** were not observed using **24f**, and equally good results were obtained at -78 or -100 °C. Overall, the use of magnesium ate reagents in these studies represents a major breakthrough as it allows reproducible preparations of key intermediates **21** and **22** and sets the stage for the synthesis of *adj*-heterocarbazoporphyrins.

Dialdehyde **21** was reacted with a dipyrromethane dicarboxylic acid **17** in the presence of catalytic TFA to give *adj*-oxacarbazoporphyrin **19** in exceptionally high yields (Scheme 5). The UV–vis spectrum of the free base **19** shows a broad Soret-type band at 430 nm with a secondary absorption band at 371 nm, and Q-like bands are present between 500 and 700 nm (Figure 4). Addition of trace amounts of TFA resulted in the formation of monocation **19H**⁺, which showed a series of absorptions with two intense bands at 394 and 438 nm, followed by Q-type bands between 530 and 800 nm. However, further addition of TFA led to additional changes in the UV–vis spectra demonstrating the formation of a new species. In neat TFA, a strong Soret band was observed at 421 nm, followed by several Q bands culminating in a relatively strong absorption at 680 nm. These bands were

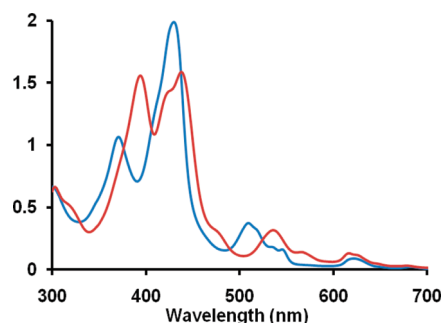


FIGURE 4. UV–vis spectra of oxacarbazoporphyrin **19**. Blue line: free base in 1% Et₃N–chloroform. Red line: monocation **19H**⁺ in 1% TFA–chloroform.

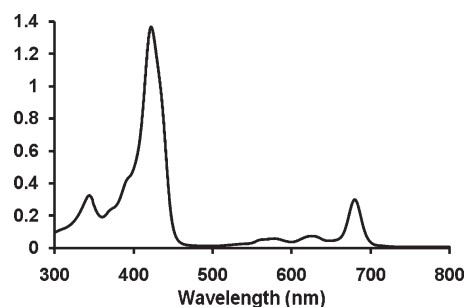


FIGURE 5. UV–vis spectrum of dication **19H**₂²⁺ in 1% HCl–TFA.

strengthened in 1% concd HCl–TFA (Figure 5), although they are otherwise essentially unchanged, indicating that a new dicationic species **19H**₂²⁺ can only be fully generated in highly acidic media.

Porphyrin analogue **19** can potentially exist in two tautomeric forms, **19a** and **19b**, although these cannot be distinguished by standard spectroscopic techniques (Scheme 5). The 500 MHz proton NMR spectrum for **19** exhibits strongly diatropic characteristics (Figure 6), where the internal CH gives a resonance upfield at -5.73 ppm and the NH appears at -3.08 ppm, while the external *meso*-protons show up as four 1H singlets in the range of 9.65–10.12 ppm. The substituents directly attached to the periphery of the macrocycle also show significant downfield shifts, e.g., where the methyl groups give rise to two 3H singlets at 3.47 and 3.49 ppm. Nevertheless, these shifts are slightly reduced compared to the values reported for benzocarbazoporphyrins **3**.⁷ Addition of a drop of TFA gave the monocation **19H**⁺ (Scheme 6), and this showed an increased ring current where the range of chemical shift values, $\Delta\delta$, increased from 15.85 to 18.09 ppm (Figure 6). The CH resonance shifted downfield to -7.81 ppm, while two separate NH peaks could be seen at -5.64 and -5.42 ppm. The *meso*-protons now show up in the range of 9.88–10.28 ppm, and this downfield shift is echoed for the methyl groups, which show up as singlets at 3.56 and 3.68 ppm. Surprisingly, the proton NMR spectrum of the dicationic form **19H**₂²⁺ showed an even stronger diatropic ring current (Figure 6). This spectrum was obtained in TFA containing several drops of concd HCl, as TFA alone was insufficient to completely generate the dication from monocation **19H**⁺. The *meso*-protons for the dication gave rise to four 1H singlets at 11.92, 11.90, 11.36, and 11.13 ppm, while the protons on the internal sp³ hybridized carbon for the indene subunit were seen as a singlet at -5.67 ppm. Two

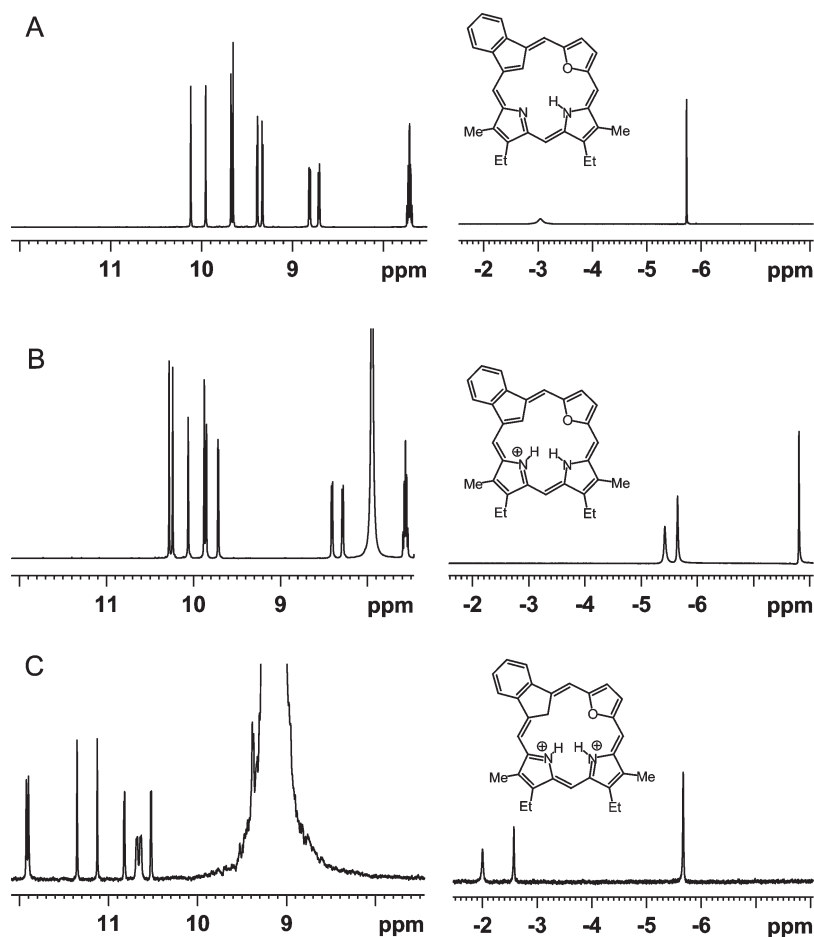
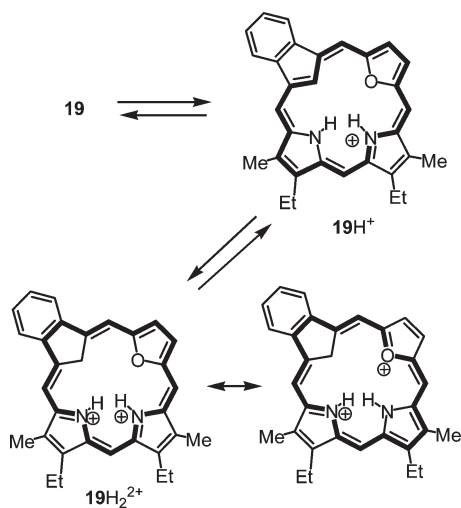


FIGURE 6. 500 MHz proton NMR spectra of oxocarbaporphyrin **19** showing the upfield and downfield regions. (A) Free base in CDCl_3 . (B) Monocation 19H^+ in TFA-CDCl_3 . (C) Dication 19H_2^{2+} in TFA containing several drops of concd hydrochloric acid. A small sealed capillary tube containing C_6D_6 was used as a reference.

SCHEME 6



NH singlets were observed at -2.00 and -2.57 ppm, while the methyl protons were shifted downfield to 4.02 and 3.98 ppm. The protons on the furan subunit were also pushed further downfield to give two 1H doublets at 10.52 and 10.82 ppm. As we have noted previously,⁴ aromatic delocalization

pathways often aid in charge delocalization, and this factor appears to play a role in enhancing the diatropicity of these protonated species.

Addition of 1–2 drops of *d*-TFA to NMR solutions of **19** in CDCl_3 showed the immediate loss of signal intensity for the internal CH and NH resonances, showing that rapid proton exchange had occurred. This indicates that the monocation is in equilibrium with the C-protonated dicationic form 19H_2^{2+} (Scheme 6). However, no significant exchange was seen at the *meso*-positions even after a period of several days, although benzocarbaporphyrins **3** do show exchange at these positions.^{7d} This difference may be due to the reduced ability of oxygen, compared to nitrogen, to stabilize the positive charge in the C-protonated species. Similar observations were made for the isomeric oxocarbaporphyrin **12a**.²³

Oxocarbaporphyrin **19** gave crystals that were suitable for X-ray diffraction analysis by vapor diffusion into chloroform. The single crystal X-ray structure confirmed the identity of **19** and illustrated that the macrocycle is remarkably planar (Figure 7). This is evidenced by the distances (0.069 Å rms; C(2b), $0.17(3)$ Å max) skeletal atoms lie from the plane defined by C(21)O(22)N(23)N(24) and by the dihedral angles of the component indene, furan, N(23) pyrrole, and N(24) pyrrole rings relative to the mean [18]annulene plane, which were $1.37(6)^\circ$, $2.6(1)^\circ$, $1.5(1)^\circ$, and $4.0(1)^\circ$ respectively.

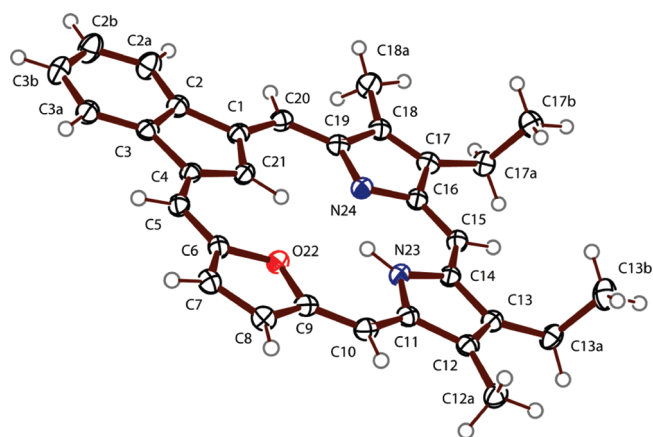
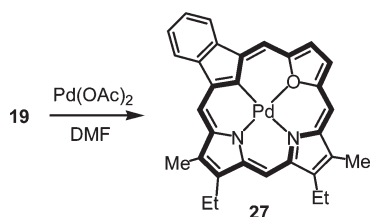


FIGURE 7. ORTEP III drawing (50% probability level, hydrogen atoms drawn arbitrarily small) of **19**. Selected bond lengths (Å): C(1)–C(2) 1.480(2), C(2)–C(3) 1.412(3), C(3)–C(4) 1.478(2), C(4)–C(5) 1.393(3), C(5)–C(6) 1.386(2), C(6)–C(7) 1.399(3), C(7)–C(8) 1.372(3), C(8)–C(9) 1.401(3), C(9)–C(10) 1.384(3), C(10)–C(11) 1.388(3), C(11)–C(12) 1.444(2), C(12)–C(13) 1.370(3), C(13)–C(14) 1.438(2), C(14)–C(15) 1.386(3), C(15)–C(16) 1.400(2), C(16)–C(17) 1.466(3), C(17)–C(18) 1.359(3), C(18)–C(19) 1.463(3), C(19)–C(20) 1.399(3), C(20)–C(1) 1.394(3), C(4)–C(21) 1.402(3), C(21)–C(1) 1.402(3), C(6)–O(22) 1.390(2), C(9)–O(22) 1.383(2), C(11)–N(23) 1.380(2), C(14)–N(23) 1.374(2), C(16)–N(24) 1.357(2), C(19)–N(24) 1.368(2).

SCHEME 7



The free base exists as a single tautomer where the NH is at position 23 and therefore corresponds to tautomer **19a** (Scheme 5). This structure is equivalent to the less stable tautomer **6b** (Figure 2) in the theoretical study,¹⁴ but as the predicted difference in energy was only 1 kcal/mol this may not be particularly significant. However, the geometry of tautomer **19a** appears to be more favorable for hydrogen bonding interactions, and there are reduced steric interactions in the macrocyclic cavity, so a naïve analysis would favor **19a** over **19b** in any case. The bond lengths obtained from the X-ray structure are consistent with the presence of a significant 18 π electron delocalization pathway, and the shorter bond length for C17–C18 compared to C12–C13 indicates that this bond has more double bond character. The absence of significant bond length alternation is also consistent with an aromatic system.

Carbaporphyrins have previously been shown to form stable organometallic derivatives.^{11,12} In addition, *opp*-oxacarbaporphyrin **12** formed stable metal complexes with nickel(II), palladium(II), and platinum(II) salts (Scheme 1), and we speculated that similar organometallic products could be prepared from **19**. When **19** was heated with palladium(II) acetate in DMF, the metallo-derivative **27** was obtained in excellent yields (Scheme 7). The proton NMR spectrum of the palladium complex (Figure 8) shows a slightly reduced ring current compared to the free base **19**

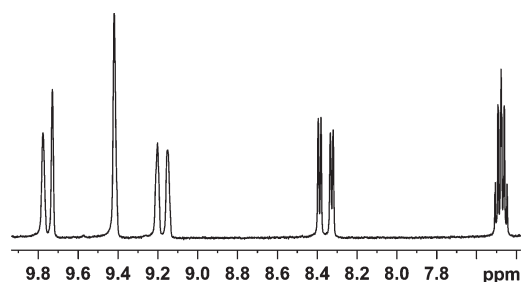


FIGURE 8. Downfield region of the 500 MHz proton NMR spectrum for palladium(II) complex **27** in CDCl_3 .

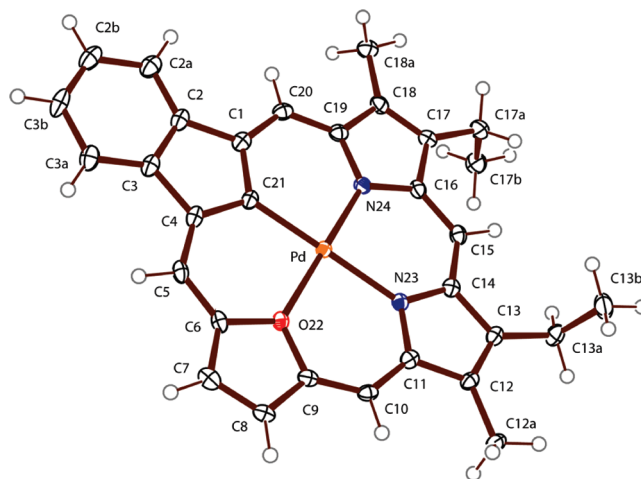


FIGURE 9. ORTEP III drawing (50% probability level, hydrogen atoms drawn arbitrarily small) of **27**. Selected bond lengths (Å): C(1)–C(2) 1.478(4), C(2)–C(3) 1.404(4), C(3)–C(4) 1.486(4), C(4)–C(5) 1.388(4), C(5)–C(6) 1.377(4), C(6)–C(7) 1.384(4), C(7)–C(8) 1.374(4), C(8)–C(9) 1.391(4), C(9)–C(10) 1.379(4), C(10)–C(11) 1.385(4), C(11)–C(12) 1.453(4), C(12)–C(13) 1.359(4), C(13)–C(14) 1.455(4), C(14)–C(15) 1.385(4), C(15)–C(16) 1.392(4), C(16)–C(17) 1.446(4), C(17)–C(18) 1.361(4), C(18)–C(19) 1.440(4), C(19)–C(20) 1.388(4), C(20)–C(1) 1.375(4), C(4)–C(21) 1.417(4), C(21)–C(1) 1.416(4), C(6)–O(22) 1.405(3), C(9)–O(22) 1.409(3), C(11)–N(23) 1.369(3), C(14)–N(23) 1.365(3), C(16)–N(24) 1.380(3), C(19)–N(24) 1.379(3), Pd–C(21) 1.968(3), Pd–O(22) 2.146(2), Pd–N(23) 2.058(2), Pd–N(24) 2.000(2). Selected bond angles (deg): C(21)–Pd–O(22) 90.06(10), O(22)–Pd–N(23) 88.77(8), N(23)–Pd–N(24) 91.17(9), C(21)–Pd–N(24) 90.0(1), C(21)–Pd–N(23) 178.74(11), O(22)–Pd–N(24) 179.67(8).

where the four *meso*-protons gave rise to three singlets in the range of 9.42–9.78 ppm. The protons on the furan ring were poorly resolved showing broad singlets at 9.15 and 9.20 ppm, upfield from the values noted for **19**, and the methyl groups also shifted upfield to give two 3H singlets at 3.26 and 3.43 ppm. The UV–vis spectrum of the palladium complex **27** showed two strong bands at 405 and 462 nm, with weaker Q-type bands between 520 and 657 nm. The metallo-derivative was further characterized by carbon-13 NMR spectroscopy and mass spectrometry. Unfortunately, all attempts to prepare the nickel(II) complex of **19** have so far been unsuccessful.

The identity of the palladium complex **27** and the planarity of the macrocycle were confirmed by single crystal X-ray analysis (Figure 9). Crystals for the X-ray diffraction analysis were obtained by vapor diffusion of hexanes into chloroform. As expected, **27** has a near planar macrocyclic core

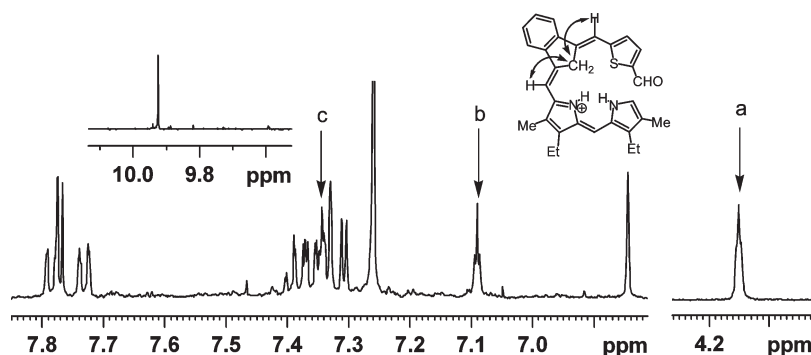
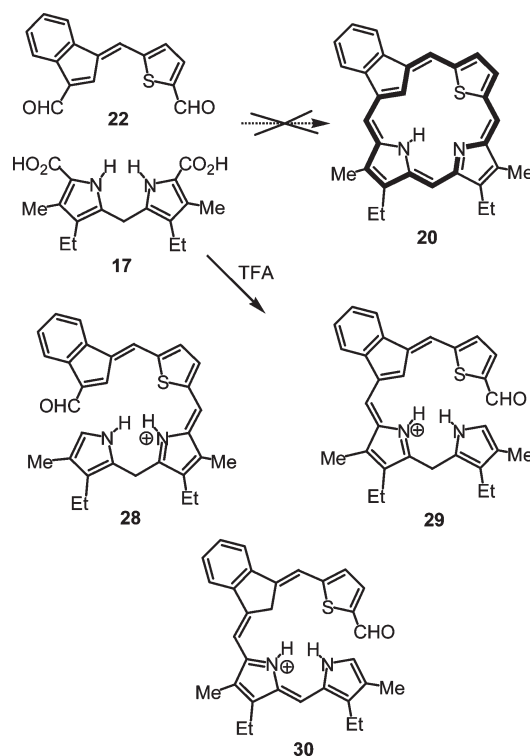


FIGURE 10. Partial 500 MHz proton NMR spectrum for a crude sample of open-chain monoaldehyde **30** in CDCl_3 . The long-range coupled triplets labeled as “a” (2H), “b” (1H), and “c” (1H) correspond to the $-\text{CH}=\text{C}-\text{CH}_2-\text{C}=\text{CH}-$ unit for the indene and the surrounding methines.

evidenced by the distances (0.076 \AA rms; 0.19 \AA max, C(2b)) skeletal atoms lie from the plane defined by Pd(1)C(21)O-(22)N(23)N(24) and by the dihedral angles of the component indene, furan, N(23) pyrrole, and N(24) pyrrole rings relative to the mean [18]annulene plane, which were $2.4(1)^\circ$, $1.4(1)^\circ$, $0.6(1)^\circ$, and $3.6(1)^\circ$ respectively. Again the bond lengths were consistent with an aromatic 18π electron delocalization system. The Pd–N23 bond length of $2.058(2) \text{ \AA}$ is significantly longer than the Pd–N24 bond length of $2.000(2)$, and this is consistent with the *trans* effect due to the more Lewis basic alkenyl unit.^{12a} In fact, the Pd–N23 bond length is more than 2σ larger than the typical $2.012 \pm 0.018 \text{ \AA}$ value reported for palladium coordinated porphyrin-type macrocycles.²³ In **27**, the Pd–O bond length is 2.146 \AA compared to 2.188 \AA in **13b**; again the longer bond length in **13b** is consistent with the same *trans* effect.

Given the excellent results obtained in the synthesis of **19**, it was anticipated that good results would also be obtained in the synthesis of thia-analogue **20**. However, when dialdehyde **22** was reacted with dipyrromethane **17** in presence of TFA in dichloromethane, no evidence for the formation of the macrocycle **20** was obtained. The use of other acid catalysts such as HBr or HCl also failed to give any porphyrinoid product. Nevertheless, the formation of partially condensed products was noted. These open-chain structures were somewhat unstable, particularly under basic or neutral conditions. Prolonged reaction times ($> 16 \text{ h}$) primarily gave one product, but at earlier reaction times a mixture of two species was isolated. Initial reaction between **17** and **22** could give rise to two regioisomeric conjugated monoaldehydes **28** and **29**. ESI and FAB MS gave a molecular ion of m/z 479, which is consistent with both of these protonated open-chain bilin analogues. In addition, high resolution ESI MS also gave m/z 479.2157 for this species, which fits the expected molecular formula $\text{C}_{31}\text{H}_{31}\text{O}^+$. However, the proton NMR spectrum for the product isolated for longer time reactions was not consistent with either of these structures. In addition to the ^1H singlet for the aldehyde moiety at 9.92 ppm , the proton NMR spectrum showed a long-range coupled system with triplets at 4.15 (2H), 7.09 (1H) and 7.34 ppm (1H), interactions that were confirmed by $^1\text{H}-^1\text{H}$ COSY. These data imply that allylic coupling is occurring over a $-\text{CH}=\text{C}-\text{CH}_2-\text{C}=\text{CH}-$ unit, and this in turn indicates that the condensation product is the fully conjugated bilin analogue **30** (Figure 10). Although steric factors may be partially responsible for the failure of this species to cyclize to give a macrocyclic product,

SCHEME 8



the positive charge in **30** is delocalized over the whole system, and this would not favor electrophilic attack onto the aldehyde group. The NMR spectra at earlier times showed a second aldehyde in addition to **30**, and these data are consistent with the presence of either **28** or **29** (Scheme 8). It is worth noting that **30** is a tautomer of **29**, and a mixture of these two species would make sense only if the rate of tautomerization was very slow. As the second open-chain species disappears in later time experiments, it could be concluded that **29** is converted into **30**. However, the results also could indicate that **28** is the second species and that it gradually decomposes or forms oligomeric byproduct. As there is no reason to think that the tautomerization of **29** to **30** would be a slow process, the latter interpretation is more likely.

The synthesis of porphyrin analogues also relies on the fulvenes taking on the correct geometry for macrocycle formation to occur. In order to assess this factor, a single crystal X-ray diffraction study was conducted on dialdehyde **22**.

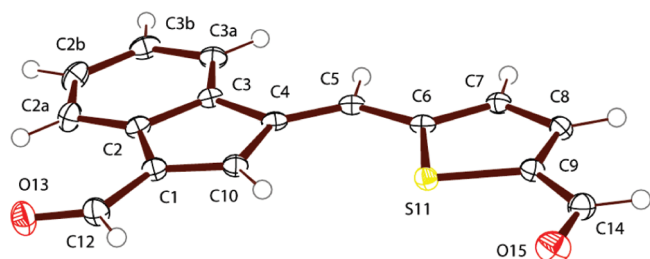


FIGURE 11. ORTEP III drawing (50% probability level, hydrogen atoms drawn arbitrarily small) of fulvene dialdehyde **22**.

Suitable crystals were obtained by vapor diffusion of hexane into chloroform, and the data showed that **22** was near planar (Figure 11) and has the required conformation across the bridge to make it a suitable intermediate for the formation of porphyrinoid products. Although it is not clear why this fulvene does not afford the macrocyclic system, the increased steric barrier to macrocyclization due to the sulfur⁴⁰ and the indene methylene unit and the decreased reactivity of the conjugated bilin analogue must play significant roles.

Conclusion

The first example of a 22-oxacarba porphyrin has been synthesized in excellent yields by a MacDonald “2 + 2” approach using a fulvene dialdehyde as the key intermediate. This new porphyrin analogue shows strongly diatropic character that is enhanced upon protonation with TFA. In HCl–TFA, a dicationic species is generated that shows a particularly strong diatropic ring current and a recognizably porphyrin-like UV–vis spectrum. The macrocycle also readily formed a palladium(II) organometallic complex, although this species showed slightly reduced diatropicity. However, attempts to prepare a related thiacarba porphyrin using the same methodology were thwarted, possible in part because of steric interactions. Although no macrocyclic products were formed, an unstable open-chain species was isolated instead. NMR data and mass spectrometry allowed this species to be assigned as an open-chain bilin analogue. These observations give valuable insights into the requirements for macrocycle formation, as well as providing a versatile route to 22-oxacarba porphyrins.

Experimental Section

1-(2-Furylmethylene)indene-3-carbaldehyde (23a). Di-*n*-butylboron triflate (1.0 M in dichloromethane, 600 μ L) was added to a stirred solution of furfural (100 mg, 1.04 mmol) in dichloromethane (150 mL). A solution of indene enamine **15**⁴¹ (195.8 mg, 1.14 mmol) in dichloromethane (150 mL) was then added dropwise over 10 min, and the resulting solution was stirred at room temperature overnight. Saturated sodium acetate solution (70 mL) was added, and the mixture was allowed to stir for 10 min. The product was extracted with dichloromethane, and the extract was washed with saturated sodium bicarbonate and then with brine. The organic phase was dried over sodium sulfate, the solvent was removed under reduced pressure, and the residue was purified by flash chromatography on silica eluting with 50% hexanes–dichloromethane. Recrystallization with chloroform–hexanes gave the fulvene aldehyde (131.8 mg, 0.59 mmol, 57%) as dark brown crystals, mp 110–112 °C;

¹H NMR (500 MHz, CDCl₃) δ 6.60 (1H, dd, J = 1.8, 3.5 Hz), 6.84 (1H, d, J = 3.5 Hz), 7.27–7.34 (2H, m), 7.33 (1H, s), 7.64–7.66 (1H, m), 7.70 (1H, d, J = 1.8 Hz), 8.08–8.10 (1H, m), 8.12 (1H, s), 10.25 (1H, s); ¹³C NMR (125 MHz, CDCl₃) δ 113.3, 118.9, 119.4, 120.2, 123.1, 126.5, 129.0, 134.8, 137.4, 137.7, 141.4, 142.0, 146.9, 153.2, 189.3; HRMS (EI) m/z calcd for C₁₅H₁₀O₂ 222.0683, found 222.0681.

1-(5-Bromo-2-furylmethylene)indene-3-carbaldehyde (23b). 5-Bromo-2-furaldehyde (182 mg, 1.04 mmol) and indene enamine **15**⁴¹ (195.8 mg; 1.14 mmol) were reacted for 40 h in the presence of dibutylboron triflate (1.0 M in dichloromethane; 600 μ L) using the foregoing conditions. Recrystallization with chloroform–hexanes gave the fulvene aldehyde (162.2 mg, 0.54 mmol, 52%) as red crystals, mp 152 °C; ¹H NMR (500 MHz, CDCl₃) δ 6.52 (1H, d, J = 3.5 Hz), 6.76 (1H, d, J = 3.5 Hz), 7.18 (1H, s), 7.26–7.34 (2H, m), 7.60–7.62 (1H, m), 7.98 (1H, s), 8.07–8.09 (1H, m), 10.21 (1H, s); ¹³C NMR (125 MHz, CDCl₃) δ 115.3, 118.6, 119.4, 120.4, 123.3, 126.7, 127.9, 128.2, 135.1, 137.4, 137.5, 140.4, 142.4, 154.8, 189.4; HRMS (EI) m/z calcd for C₁₅H₉O₂Br 299.9783, found 299.9786. Anal. Calcd for C₁₅H₉O₂Br: C, 59.83; H, 3.01. Found: C, 59.94; H, 2.78.

1-(5-Iodo-2-furylmethylene)indene-3-carbaldehyde (23c). 5-Iodo-2-furaldehyde⁴² (229 mg, 1.04 mmol) and indene enamine **15**⁴¹ (195.8 mg; 1.14 mmol) were reacted for 40 h in the presence of dibutylboron triflate (1.0 M in dichloromethane; 600 μ L) using the previously described conditions. Recrystallization with chloroform–hexanes gave the fulvene aldehyde (173.4 mg, 0.50 mmol, 48%) as orange crystals, mp 150 °C, dec; ¹H NMR (500 MHz, CDCl₃) δ 6.69 (1H, d, J = 3.6 Hz), 6.74 (1H, d, J = 3.6 Hz), 7.20 (1H, s), 7.26–7.33 (2H, m), 7.60–7.62 (1H, m), 7.99 (1H, s), 8.08–8.10 (1H, m), 10.21 (1H, s); ¹³C NMR (125 MHz, CDCl₃) δ 94.9, 118.3, 119.5, 120.6, 123.3, 124.0, 126.7, 128.3, 135.4, 137.4, 137.5, 140.0, 142.4, 158.1, 189.4; HRMS (EI) m/z calcd for C₁₅H₉O₂I 347.9645, found 347.9648. Anal. Calcd for C₁₅H₉O₂I: C, 51.75; H, 2.61. Found: C, 51.90; H, 2.50.

1-(2-Thienylmethylene)indene-3-carbaldehyde (23d). 2-Thiophenecarbaldehyde (117 mg, 1.04 mmol) and indene enamine **15**⁴¹ (195.8 mg, 1.14 mmol) were reacted in the presence of dibutylboron triflate (1.0 M in dichloromethane, 600 μ L) by the procedure described above. The crude product was purified flash chromatography on silica eluting with 50% hexanes–dichloromethane. The solvent was removed under reduced pressure and the residue was treated with chloroform–hexanes. The fulvene aldehyde (141 mg, 0.59 mmol, 57%) was isolated as a dark brown oil. ¹H NMR (500 MHz, CDCl₃) δ 7.15 (1H, dd, J = 3.6, 5.1 Hz), 7.28–7.34 (2H, m), 7.41–7.43 (1H, m), 7.57–7.59 (1H, m), 7.65–7.67 (1H, m), 7.78 (1H, d, J = 0.6 Hz), 7.86 (1H, d, J = 0.6 Hz), 8.08–8.10 (1H, m), 10.18 (1H, s); ¹³C NMR (125 MHz, CDCl₃) δ 113.3, 118.9, 119.4, 120.2, 123.1, 126.5, 129.0, 134.8, 137.4, 137.7, 141.4, 142.0, 146.9, 153.2, 189.3; HRMS (EI) m/z calcd for C₁₅H₁₀OS 238.0452, found 238.0452.

1-(5-Bromo-2-thienylmethylene)indene-3-carbaldehyde (23e). 5-Bromo-2-thiophenecarbaldehyde (198 mg, 1.04 mmol) and indene enamine **15**⁴¹ (195.8 mg, 1.14 mmol) were reacted for 40 h in the presence of dibutylboron triflate (1.0 M in dichloromethane, 600 μ L) using the foregoing conditions. Recrystallization from chloroform–hexanes gave the fulvene aldehyde (185 mg, 0.59 mmol, 56%) as bright orange crystals, mp 172–174 °C; ¹H NMR (500 MHz, CDCl₃) δ 7.11 (1H, d, J = 4.0 Hz), 7.15 (1H, d, J = 4.0 Hz), 7.27–7.34 (2H, m), 7.63 (1H, s), 7.63–7.65 (1H, m), 7.70 (1H, s), 8.06–8.08 (1H, m), 10.17 (1H, s); ¹³C NMR (125 MHz, CDCl₃) δ 119.4, 119.6, 123.4, 126.92, 126.94, 128.2, 131.4, 134.4, 135.9, 137.3, 137.8, 138.0, 141.7, 142.8, 189.0; HRMS (EI) m/z calcd for C₁₅H₉BrOS 315.9558, found 315.9557. Anal. Calcd for C₁₅H₉BrOS: C, 56.80; H, 2.86; Found: C, 56.43; H, 2.73.

(40) Armiger, Y.-L. S. T.; Lash, T. D. *J. Heterocycl. Chem.* **1992**, 29, 523–527.

(41) Arnold, Z. *Collect. Czech. Chem. Commun.* **1965**, 30, 2783–2792.

(42) Mocelo, R.; Pustovarov, V. *Rev. Deriv. Cana Azucar* **1975**, 9, 29–37.

1-(5-Iodo-2-thienylmethylene)indene-3-carbaldehyde (23f). 5-Iodo-2-thiophenecarbaldehyde⁴³ (248 mg, 1.04 mmol) and indene enamine **15**⁴¹ (195.8 mg, 1.14 mmol) were reacted for 40 h in the presence of dibutylboron triflate (1.0 M in dichloromethane, 600 μ L) using the foregoing conditions. Recrystallization from chloroform–hexanes gave the fulvene aldehyde (166 mg, 0.46 mmol, 44%) as bright red crystals, mp 180 °C, dec; ¹H NMR (500 MHz, CDCl₃) δ 7.06 (1H, d, J = 3.8 Hz), 7.28–7.34 (3H, m), 7.64–7.66 (1H, m), 7.69 (1H, s), 7.74 (1H, s), 8.07–8.09 (1H, m), 10.19 (1H, s); ¹³C NMR (125 MHz, CDCl₃) δ 81.8, 119.5, 123.4, 126.4, 126.9, 128.3, 135.3, 136.3, 137.3, 137.8, 138.2, 138.3, 142.9, 146.1, 189.1; HRMS (EI) m/z calcd for C₁₅H₉IOS 363.9419, found 363.9419. Anal. Calcd for C₁₅H₉IOS: C, 49.47; H, 2.49. Found: C, 49.42; H, 2.35.

1-(5-Formyl-2-furylmethylene)indene-3-carbaldehyde (21). Fulvene **23c** (100 mg, 0.29 mmol), trimethyl orthoformate (2.5 mL), and dichloromethane (30 mL) were added to a round-bottomed flask equipped with a drying tube. Next, cerium chloride heptahydrate (270 mg) and methanol (80 mL) were added, and the contents of the flask were refluxed for 2 h. The reaction was quenched with saturated sodium bicarbonate solution (40 mL). The product was extracted with dichloromethane and dried over sodium sulfate. The solvent was evaporated under reduced pressure, and the residue was recrystallized with chloroform–hexanes to give the protected fulvene **143** (98 mg, 0.25 mmol, 87%) as an orange solid. ¹H NMR (500 MHz, CDCl₃) δ 3.42 (6H, s), 5.54 (1H, d, J = 0.5 Hz), 6.56 (1H, d, J = 3.6 Hz), 6.67 (1H, d, J = 3.6 Hz), 7.00 (1H, s), 7.18–7.26 (1H, m), 7.31–7.32 (1H, m), 7.50–7.53 (1H, m), 7.55–7.58 (1H, m). The product was somewhat unstable and was taken on without further purification.

To a 100 mL three-necked round-bottom flask fitted with a thermometer, drying tube, and rubber septum was added *n*-BuMgCl (0.58 mL, 2.0 M solution in THF) in ether (10 mL), followed by the addition of *n*-BuLi (1.5 mL, 1.6 M solution in hexanes), and the mixture was stirred for 10 min at 0 °C. The mixture was cooled to –100 °C, and a solution of protected fulvene **24c** (100 mg, 0.25 mmol) in ether (20 mL) was added dropwise. The mixture was allowed to react at –100 °C for 45 min. DMF (0.5 mL) was added to the cooled mixture, the cooling bath was removed, and the mixture was allowed to warm to room temperature and stirred for a further 2 h. The reaction was quenched with 10% HCl and washed with saturated ammonium chloride solution. The product was extracted with dichloromethane and dried over sodium sulfate, and the solvent was removed under reduced pressure. The residue was purified by flash chromatography on silica eluting with 1% methanol–dichloromethane. Recrystallization with chloroform–hexanes gave the fulvene dialdehyde (29 mg, 0.12 mmol, 46%) as an orange solid, mp 132 °C; ¹H NMR (500 MHz, CDCl₃) δ 6.91 (1H, d, J = 3.8 Hz), 7.27–7.36 (4H, m), 7.63–7.65 (1H, m), 8.05–8.07 (1H, m), 8.07 (1H, s), 9.77 (1H, s), 10.24 (1H, s); ¹³C NMR (125 MHz, CDCl₃) δ 118.0, 118.7, 120.1, 122.6, 123.7, 127.2, 129.3, 137.1, 138.0, 139.8, 140.2, 144.0, 154.3, 156.8, 177.6, 189.5; HRMS (EI) m/z calcd for C₁₆H₁₀O₃ 250.0631, found 250.0630. Anal. Calcd for C₁₆H₁₀O₃: C, 76.79; H, 4.03. Found: C, 76.43; H, 3.90.

1-[5-(3-Oxo-2-propyl-1-propenyl)-2-furylmethylene]indene-3-carbaldehyde (26). To a 100 mL three-necked round-bottom flask fitted with a thermometer, drying tube, and rubber septum was added *n*-BuMgCl (0.58 mL, 2.0 M solution in THF) in ether (10 mL), followed by the addition of *n*-BuLi (2.0 mL, 1.6 M solution in hexanes), and the mixture was stirred for 10 min at 0 °C. After the mixture was cooled to –70 °C, a solution of protected fulvene **24c** (100 mg, 0.25 mmol) in ether (20 mL) was added dropwise. The mixture was allowed to react at this temperature for 45 min. DMF (0.5 mL) was added while

maintaining the temperature at –70 °C, and the mixture was allowed to warm to room temperature and further stirred for 2 h. The reaction was quenched with 10% HCl and washed with saturated ammonium chloride solution. The product was extracted with dichloromethane and dried over sodium sulfate, and the solvent removed under reduced pressure. The residue was purified on a silica gel flash column eluting with 1% methanol–dichloromethane. The first band, which contained the title dialdehyde, was followed by a second fraction corresponding to **21**. Recrystallization of **26** with chloroform–hexanes gave the fulvene dialdehyde byproduct (15 mg, 0.047 mmol, 19%) as an orange solid, mp 148 °C; ¹H NMR (500 MHz, CDCl₃) δ 1.03 (3H, t, J = 7.4 Hz), 1.57–1.67 (2H, m), 2.78 (2H, t, J = 7.8 Hz), 6.92 (1H, d, J = 3.8 Hz), 6.97 (1H, d, J = 3.8 Hz), 7.06 (1H, s), 7.29–7.36 (2H, m), 7.32 (1H, s), 7.65–7.67 (1H, m), 8.05 (1H, s), 8.08–8.10 (1H, m), 9.58 (1H, s), 10.23 (1H, s); ¹³C NMR (125 MHz, CDCl₃) δ 14.5, 21.7, 27.3, 118.8, 119.4, 121.1, 123.5, 126.9, 128.6, 133.8, 136.8, 137.4, 137.6, 139.7, 142.1, 142.8, 154.99, 155.05, 189.0, 194.0; HRMS (EI) m/z calcd for C₂₁H₁₈O₃ 318.1254, found 318.1256.

1-(5-Formyl-2-thienylmethylene)indene-3-carbaldehyde (22). Fulvene **23f** (100 mg, 0.27 mmol), trimethyl orthoformate (2.5 mL), and dichloromethane (30 mL) were added to a round-bottomed flask equipped with a drying tube. Next, cerium(III) chloride heptahydrate (270 mg) and methanol (80 mL) were added, and the contents of the flask were refluxed for 2 h. The reaction was quenched with saturated sodium bicarbonate solution (40 mL). The product was extracted with dichloromethane and dried over sodium sulfate. The solvent was evaporated under reduced pressure, and the residue was recrystallized from chloroform–hexanes to give the protected fulvene **24f** (100 mg, 0.24 mmol, 90%) as an unstable orange-brown solid. ¹H NMR (500 MHz, CDCl₃) δ 3.39 (6H, s), 5.53 (1H, d, J = 1.1 Hz), 6.95 (1H, dd, J = 0.5, 3.8 Hz), 7.14 (1H, br t, J = 0.9 Hz), 7.19–7.25 (3H, m), 7.42 (1H, s), 7.48–7.51 (1H, m), 7.59–7.61 (1H, m); ¹³C NMR (125 MHz, CDCl₃) δ 52.8, 78.5, 100.1, 119.2, 120.3, 121.1, 124.1, 125.8, 127.8, 132.8, 136.8, 137.7, 138.2, 139.9, 144.6, 146.8; HRMS (EI) m/z calcd for C₁₇H₁₃IO₂S 409.9838, found 409.9834.

To a 100 mL three-necked round-bottom flask fitted with a thermometer, drying tube, and rubber septum was added *n*-BuMgCl (0.58 mL, 2.0 M solution in THF) in ether (10 mL), followed by the addition of *n*-BuLi (1.5 mL, 1.6 M solution in hexanes), and the mixture was stirred for 10 min at 0 °C. The mixture was cooled to –100 °C, and a solution of protected fulvene **24f** (100 mg, 0.24 mmol) in ether (20 mL) was added dropwise. The mixture was allowed to react at this temperature for 45 min. DMF (0.50 mL) was added to the solution at –100 °C. The mixture was allowed to warm to room temperature, and stirring was continued for 2 h. The reaction was quenched with 10% HCl and washed with saturated ammonium chloride solution. The product was extracted with dichloromethane and dried over sodium sulfate, and the solvent was removed under reduced pressure. The residue was purified by flash chromatography on silica eluting with dichloromethane. Recrystallization with chloroform–hexanes gave the fulvene dialdehyde (40 mg, 0.15 mmol, 63%) as a bright orange solid, mp 203–205 °C; ¹H NMR (500 MHz, CDCl₃) δ 7.29–7.36 (2H, m), 7.46 (1H, d, J = 3.8 Hz), 7.66–7.68 (1H, m), 7.72 (1H, s), 7.76 (1H, d, J = 3.8 Hz), 7.83 (1H, s), 8.05–8.07 (1H, m), 9.96 (1H, s), 10.20 (1H, s); ¹³C NMR (125 MHz, CDCl₃) δ 120.1, 123.7, 126.0, 127.4, 129.1, 133.8, 136.4, 137.4, 137.7, 137.7, 139.9, 144.1, 146.8, 147.8, 182.9, 189.1; HRMS (EI) m/z calcd for C₁₆H₁₀O₂S 266.0402, found 266.0402. Anal. Calcd for C₁₆H₁₀O₂S: C, 72.16; H, 3.78. Found: C, 71.70; H, 3.64.

13,17-Diethyl-12,18-dimethyl-21-carba-22-oxabenzob[*b*]porphyrin (19). Dipyrromethane dicarboxylic acid **17**³⁰ (38 mg, 0.12 mmol) was stirred with 5 mL of TFA under nitrogen for 2 min. The solution was diluted with dichloromethane (100 mL), and

(43) De Sousa, P. T., Jr.; Taylor, R. J. K. *Synlett* **1990**, 755–757.

fulvene dialdehyde **21** (30 mg, 0.12 mmol) in 50 mL of dichloromethane was added immediately. The solution was stirred under nitrogen at room temperature overnight. The solution was then washed with water and saturated sodium bicarbonate solution, and the solvent was removed under reduced pressure. The residue was purified by column chromatography on grade 3 alumina eluting with dichloromethane. Recrystallization from chloroform–hexanes gave the oxacarbaporphyrin (42 mg, 0.095 mmol, 79%) as shiny black crystals, mp > 300 °C; UV–vis (CHCl₃) λ_{max} (log ϵ) 371 (4.72), 430 (4.99), 509 (4.26), 621 nm (3.65); UV–vis (1% TFA–CHCl₃) λ_{max} (log ϵ) 303 (4.51), 394 (4.88), 438 (4.89), 536 (4.18), 617 nm (3.80); UV–vis (25% TFA–CHCl₃) λ_{max} (log ϵ) 399 (4.95), 427 (4.84), 538 (4.17), 614 (3.86), 678 nm (3.35); UV–vis (TFA) λ_{max} (log ϵ) 344 (4.49), 421 (5.12), 567 (3.70), 623 (3.80), 680 nm (4.38); UV–vis (1% concd HCl–TFA) λ_{max} (log ϵ) 344 (4.53), 422 (5.16), 579 (3.78), 625 (3.88), 680 nm (4.50); ¹H NMR (500 MHz, CDCl₃) δ –5.73 (1H, s), –3.04 (1H, br s), 1.80 (6H, t, J = 7.8 Hz), 3.47 (3H, s), 3.49 (3H, s), 3.90 (2H, q, J = 7.8 Hz), 3.95 (2H, q, J = 7.8 Hz), 7.68–7.75 (2H, m), 8.70–8.72 (1H, m), 8.80–8.82 (1H, m), 9.33 (1H, d, J = 4.4 Hz), 9.39 (1H, d, J = 4.4 Hz), 9.65 (1H, s), 9.68 (1H, s), 9.96 (1H, s), 10.12 (1H, s); ¹³C NMR (125 MHz, CDCl₃) δ 11.67, 11.74, 17.6, 17.8, 19.8, 19.9, 92.7, 97.1, 101.0, 105.5, 118.7, 120.41, 120.44, 122.9, 123.9, 126.8, 127.1, 134.6, 135.1, 136.6, 137.1, 139.9, 141.8, 142.2, 143.3, 143.4, 144.6, 148.8, 149.4, 150.5, 153.0; ¹H NMR (500 MHz, 1 drop TFA–CDCl₃; monocation **19H**⁺) δ –7.81 (1H, s), –5.64 (1H, br s), –5.42 (1H, br s), 1.79 (3H, t, J = 7.8 Hz), 1.88 (3H, t, J = 7.8 Hz), 3.56 (3H, s), 3.68 (3H, s), 4.10 (2H, q, J = 7.8 Hz), 4.19 (2H, q, J = 7.8 Hz), 7.53–7.60 (2H, m), 8.29 (1H, d, J = 6.8 Hz), 8.41 (1H, d, J = 6.8 Hz), 9.71 (1H, d, J = 4.5 Hz), 9.86 (1H, d, J = 4.5 Hz), 9.88 (1H, s), 10.06 (1H, s), 10.24 (1H, s), 10.28 (1H, s); ¹³C NMR (125 MHz, 1 drop TFA–CDCl₃) δ 11.6, 11.7, 16.9, 17.0, 20.0, 20.2, 95.2, 95.9, 104.4, 105.7, 117.8, 121.2, 121.4, 127.9, 128.8, 128.9, 129.1, 137.0, 137.2, 137.7, 138.2, 138.4, 139.3, 141.5, 141.9, 142.1, 143.1, 144.6, 152.6, 154.6; ¹H NMR (500 MHz, HCl–TFA; dication **19H**₂²⁺) δ –5.67 (2H, s), –2.57 (1H, br s), –2.00 (1H, br s), 2.09–2.16 (6H, m), 3.98 (3H, s), 4.02 (3H, s), 4.43 (2H, q, J = 7.8 Hz), 4.50 (2H, q, J = 7.8 Hz), 8.90–9.60 (2H, m), 10.52 (1H, d, J = 4.5 Hz), 10.61–10.70 (2H, m), 10.82 (1H, d, J = 4.5 Hz), 11.13 (1H, s), 11.36 (1H, s), 11.90 (1H, s), 11.92 (1H, s); HRMS (EI) m/z calcd for C₃₁H₂₈N₂O 444.2203, found 444.2202. Anal. Calcd for C₃₁H₂₈N₂O · 1/25CHCl₃: C, 82.97; H, 6.29; N, 6.29. Found: C, 83.20; H, 5.95; N, 6.23.

[13,17-Diethyl-12,18-dimethyl-21-carba-22-oxabenzob]porphyrinato]palladium(II) (27). A mixture of oxacarbaporphyrin **19** (30 mg, 0.067 mmol) and palladium acetate (18 mg, 0.080 mmol) was dissolved in DMF (20 mL) and refluxed for 2 h. The solution was then diluted with dichloromethane and washed with water, and the solution evaporated *in vacuo*. The residue was chromatographed on silica eluting with dichloromethane, and a dark brown fraction was collected. Recrystallization from chloroform–hexanes gave **27** (29.4 mg, 0.067 mmol, 80%) as shiny black crystals, mp > 300 °C; UV–vis (CHCl₃) λ_{max} (log ϵ) 405 (4.68), 439 (4.57), 462 (4.67), 520 (4.13), 555 (3.90), 599 (3.51), 657 nm (3.58); ¹H NMR (500 MHz, CDCl₃) δ 1.75–1.80 (6H, m),

3.26 (3H, s), 3.43 (3H, s), 3.78 (2H, q, J = 7.8 Hz), 3.88 (2H, q, J = 7.8 Hz), 7.44–7.51 (2H, m), 8.33 (1H, d, J = 6.8 Hz), 8.39 (1H, d, J = 6.8 Hz), 9.15 (1H, br s), 9.20 (1H, br s), 9.42 (2H, br s), 9.73 (1H, br s), 9.78 (1H, br s); ¹³C NMR (125 MHz, CDCl₃) δ 11.3, 11.7, 17.6, 17.8, 19.7, 20.2, 93.3, 96.3, 99.6, 100.5, 108.3, 118.9, 119.2, 119.6, 120.0, 126.3, 127.1, 132.6, 133.7, 134.1, 134.2, 134.9, 140.3, 141.0, 141.2, 141.7, 141.8, 143.6, 145.9, 146.2, 147.3; HRMS (EI) m/z calcd for C₃₁H₂₆N₂OPd 548.1083, found 548.1080. Anal. Calcd for C₃₁H₂₆N₂OPd: C, 67.82; H, 4.77; N, 5.10. Found: C, 67.27; H, 4.04; N, 4.90.

Attempted Synthesis of 13,17-Diethyl-12,18-dimethyl-21-carba-22-thiabenzob]porphyrin (20). Dipyrromethane dicarboxylic acid **17** (36 mg, 0.11 mmol) was stirred with 5 mL of TFA under nitrogen for 2 min. The solution was diluted with dichloromethane (100 mL), and fulvene dialdehyde **22** (30 mg, 0.11 mmol) in dichloromethane (50 mL) was added immediately. The solution was stirred under nitrogen at room temperature overnight. The next day the solution was washed with 10% hydrochloric acid, the organic solvent was evaporated under reduced pressure, and the residue was recrystallized from chloroform–hexanes. The recrystallized material was run through a silica column, eluting with dichloromethane, and a dark brown fraction was collected. The solvent was evaporated under reduced pressure, and a black residue was obtained. ¹H NMR and COSY experiments were immediately performed, but no signs of macrocycle formation were observed. However, this product fraction corresponded instead to an unstable open chain compound, **30**. ¹H NMR (500 MHz, CDCl₃) δ 1.17–1.24 (6H, m), 2.13 (3H, s), 2.16 (3H, s), 2.61–2.70 (4H, m), 4.15 (2H, t, J = 2.0 Hz), 6.84 (1H, s), 7.09 (1H, t, J = 2.0 Hz), 7.30 (1H, d, J = 3.8 Hz), 7.33 (1H, s), 7.34 (1H, t, J = 2.0 Hz), 7.34–7.40 (2H, m), 7.72–7.74 (1H, m), 7.77 (1H, d, J = 3.8 Hz), 7.77–7.79 (1H, m), 9.92 (1H, s); HRMS (ESI) m/z calcd for C₃₁H₃₁OS 479.2158, found 479.2157.

Acknowledgment. This material is based upon work supported by the National Science Foundation under grant nos. CHE-0616555 and CHE-0911699 (to T.D.L.) and CHE-0348158 and CHE-0725294 (to G.M.F.) and by the Petroleum Research Fund, administered by the American Chemical Society. The authors thank Youngstown State University Structure & Chemical Instrumentation Facility's Matthias Zeller for X-ray data collection. The diffractometer was funded by NSF grant 0087210, Ohio Board of Regents grant CAP-491, and YSU. Funding for a 500 MHz NMR spectrometer was provided by the National Science Foundation under grant no. CHE-0722385.

Supporting Information Available: Crystallographic data for **19**, **22f**, **26**, and **27** in CIF format and experimental details for the X-ray structure determinations are provided, together with ORTEP-III figures, MS, UV–vis, ¹H NMR, and ¹³C NMR spectra for selected compounds. This material is available free of charge via the Internet at <http://pubs.acs.org>.